Harmful Algae 44 (2015) 46–53

Contents lists available at ScienceDirect

Harmful Algae

journal homepage: www.elsevier.com/locate/hal

Active role of the mucilage in the toxicity mechanism of the harmful benthic dinoflagellate *Ostreopsis* cf. *ovata*

V. Giussani [a,*], F. Sbrana [b], V. Asnaghi [a,c], M. Vassalli [b], M. Faimali [d], S. Casabianca [c,e], A. Penna [c,e], P. Ciminiello [f], C. Dell'Aversano [f], L. Tartaglione [f], A. Mazzeo [f], M. Chiantore [a,c]

[a] DISTAV – University of Genoa, corso Europa 26, 16132 Genoa, Italy
[b] CNR – The Biophysics Institute (IBF), via De Marini 6, 16149 Genoa, Italy
[c] CoNISMa – Italian Interuniversity Consortium on Marine Sciences, Piazzale Flaminio 9, 00196 Rome, Italy
[d] CNR – Institute of Marine Sciences (ISMAR), via De Marini 6, 16149 Genoa, Italy
[e] DISB – University of Urbino, via Saffi 2, 61029 Urbino, Italy
[f] University Federico II, via Montesano 49, 80131 Naples, Italy

ARTICLE INFO

Article history:
Received 11 January 2015
Received in revised form 18 February 2015
Accepted 18 February 2015
Available online

Keywords:
Ostreopsis ovata
Harmful algal blooms
Mucous
Benthic dinoflagellates
Toxicity
Atomic force microscopy (AFM)

ABSTRACT

Ostreopsis cf. *ovata* is a harmful benthic dinoflagellate, widespread along most of the Mediterranean coasts. It produces a wide range of palytoxin-like compounds and variable amounts of mucus that may totally cover substrates, especially during the stationary phase of blooms. Studies on different aspects of the biology and ecology of *Ostreopsis* spp. are increasing, yet knowledge on toxicity mechanism is still limited. In particular, the potential active role of the mucilaginous matrix has not yet been shown, although when mass mortalities have occurred, organisms have been reported to be covered by the typical brownish mucilage. In order to better elucidate toxicity dependence on direct/indirect contact, the role of the mucilaginous matrix and the potential differences in toxicity along the growth curve of *O.* cf. *ovata*, we carried out a toxic bioassay during exponential, stationary and late stationary phases. Simultaneously, a molecular assay was performed to quantify intact cells or to exclude cells presence. A liquid chromatography – high resolution mass spectrometry (LC-HRMS) analysis was also carried out to evaluate toxin profile and content in the different treatments. Our results report higher mortality of model organism, especially during the late stationary phase, when direct contact between a model organism and intact microalgal cells occurs (LC50-48h <4 cells/ml on *Artemia salina*). Also growth medium devoid of microalgal cells but containing *O.* cf. *ovata* mucilage caused significant toxic effects. This finding is also supported by chemical analysis which shows the highest toxin content in pellet extract (95%) and around 5% of toxins in the growth medium holding mucous, while the treatment devoid of both cells and mucilage did not contain any detectable toxins. Additionally, the connection between mucilaginous matrix and thecal plates, pores and trychocysts was explored by way of atomic force microscopy (AFM) to investigate the cell surface at a sub-nanometer resolution, providing a pioneering description of cellular features.

1. Introduction

In the last decade, the harmful benthic dinoflagellate *Ostreopsis* cf. *ovata* has been blooming in the Mediterranean region with increasing frequency and distribution, causing mortality of benthic organisms and with additional human health concerns (Aligizaki and Nikolaidis, 2006; Mangialajo et al., 2008; Penna et al., 2010; Rhodes, 2011; Vila et al., 2001). These events have been generated great attention on different aspects of *O.* cf. *ovata* biology (ecology, ecotoxicology, genetics, citology, etc.).

Ostreopsis genus produces palytoxin-analogs complex (PLTX) that could be involved in ciguatera fish poisoning (Tosteson, 1995; Richlen ML., 2011), a widespread form of human food poisoning caused by consumption of contaminated finfish, but further studies are required to confirm this hypothesis (Parsons et al., 2012). In particular, *O.* cf. *ovata* produces a wide range of palytoxin-like compounds: a putative palytoxin and several ovatoxins (ovatoxin–a to–f; Ciminiello et al., 2010; Guerrini et al., 2010; Ciminiello et al., 2012a, 2012b). In addition, the presence of Ostreol A, a non-palytoxin-like compound with a significant toxic effect on brine shrimp, has been recently reported (Hwang et al., 2013).

* Corresponding author. Tel.: +39 0103538563.
E-mail address: valentina.giussani@edu.unige.it (V. Giussani).

10.1016/j.hal.2015.02.006
1568-9883/

Data on the toxic effects of PLTX and some of its analogs on different model organisms have been reviewed in recent papers (Ramos and Vasconcelos, 2010; Munday, 2011). The toxin profile of *Ostreopsis* cf. *ovata* can vary but the extent to which production of these toxins is controlled by environmental versus inherent genetic differences among strains has not yet been elucidated (Pistocchi et al., 2011; GEOHAB, 2012), as well as the role of these drivers on cell proliferation and toxicity. Differently, the increasing toxins production along the growth curve of this species, reaching the maximum during the stationary phase has been proven by Guerrini et al. (2010). Similar evidences has been reported for other toxic benthic dinoflagellates (e.g. Prorocentrum lima, Gambierdiscus toxicus), which showed higher toxicity effects during stationary phase and/or the blooming phase from field samples (Grzebyk et al., 1997; Pistocchi et al., 2011; Parsons et al., 2012).

Field studies suggest that environmental variables, such as temperature and salinity, could play a key role in driving the proliferation of *Ostreopsis* spp. (Mangialajo et al., 2008; Shears and Ross, 2009; Totti et al., 2010; Mangialajo et al., 2011; Asnaghi et al., 2012; Accoroni et al., 2012). However, controversial results in different regions could be either due to different interactions among environmental drivers or different response of local strains. As a consequence, laboratory studies elucidating the role of individual environmental variables on growth and toxicity are increasing (Pistocchi et al., 2011).

Ostreopsis spp. grow attached to the substrate utilising a variable amount of mucilage in which they aggregate (Besada et al., 1982). *Ostreopsis* mucilage shows a complex structure, formed by a network of long fibers, derived from trichocysts extruded through thecal pores and by an amorphous matrix of acidic polysaccharides (Honsell et al., 2013; Escalera et al., 2014). Mucilage increases during cell proliferation in the field, producing a typical brownish mat, visible with the naked eye. Studies focusing on the mucilaginous matrix suggest its key-role in growth strategy and, possibly, in the micropredation activity of *O.* cf. *ovata* cells (Barone, 2007), defense against grazing, increased buoyancy and metabolic self-regulation (Reynolds, 2006, 2007).

An active toxicological role for the mucilaginous matrix surrounding the microalgal cells has not been shown yet, although when mass mortalities and or damage of benthic organisms have occurred (Graneli et al., 2002; Brescianini et al., 2006; Vila et al., 2008; Shears and Ross, 2010; Totti et al., 2010), organisms were reported to be covered by this typical brownish mucilage. Laboratory tests performed on juveniles and larvae of Paracentrotus lividus, also describe a mechanical impediment of model organisms due to their being wrapped in the *Ostreopsis* cf. *ovata* mucilage (Privitera et al., 2012).

A range of laboratory studies have reported much higher toxic effects on model organisms in the presence of intact *Ostreopsis* cells, compared to free cells supernatant (growth medium devoid of cells): *Artemia salina* (Faimali et al., 2012; Pezzolesi et al., 2012), *Paracentrotus lividus* (Privitera et al., 2012), sea bass juveniles (Pezzolesi et al., 2012).

In order to better elucidate toxicity dependence on direct/indirect contact, the role of the mucilaginous matrix and the potential differences in toxicity along the growth curve of *Ostreopsis* cf. *ovata*, we carried out a toxic bioassay during exponential, stationary and late stationary phases, improving the experimental design described in Faimali et al. (2012). The role of the mucilaginous matrix was investigated at the late stationary phase. In fact at this phase, concurrently with the increase of *O.* cf. *ovata* cell concentration in cultures, a larger production of mucilage matrix is observed in the external medium (Liu and Buskey, 2000; Vidyarathna and Granéli, 2012).

The experiment was mainly designed to test toxicity effects on *Artemia salina* nauplii exposed to different conditions of contact with algal cells (whole *Ostreopsis* cf. *ovata* culture; *O.* cf. *ovata* cells filtered and resuspended in fresh medium; filtered and sonicated cells; growth medium devoid of cells, but containing the mucilage; growth medium devoid of cells and of the mucilage). Concurrently, a real time PCR (qPCR) was performed to quantify intact cells or to exclude cells presence in the treatment corresponding to medium devoid of cells, but containing the mucilage. Furthermore, liquid chromatography-high resolution mass spectrometry (LC-HRMS) analyses were carried out to evaluate toxin profile and content in the different treatments.

Moreover, in order to better elucidate the functional role of the mucilaginous matrix and its links with the *Ostreopsis* cells, the connection between the thecal plates, pores, trychocysts and the mucilaginous matrix was explored by way of atomic force microscopy (AFM) to investigate cell surface at a sub-nanometer resolution, providing a pioneering description of the inner side of *O.* cf. *ovata* thecal plates.

2. Materials and methods

2.1. Ostreopsis *cf.* ovata *cultures and growth curve*

Laboratory cultures of *Ostreopsis* cf. *ovata* were obtained from environmental samples collected during the summer 2012 in Quarto dei Mille (Genoa, NW Mediterranean Sea, Italy). Cell isolation was performed at the laboratory of University of Urbino from the team of Dr. Antonella Penna (strain CBA29-2012). Algal cells were cultured into several 200 ml sterilized plastic flasks closed with transpiring caps, filled with an aliquot of *O.* cf. *ovata* culture from the masters added with filtered (GF/F 0.22 μm) sterilized marine water and Guillard growth medium F/2 (at a concentration of 1 ml L^{-1}).

At the start of the toxicity bioassay, six new flasks were prepared with initial cell concentration of 80 cells/ml. All flasks were maintained at 20 ± 0.5 °C in a 16:8 h light:dark (L:D) cycle (light intensity 85–135 μE m^{-2} s^{-1}). To set up the growth curve, cell counts were performed in triplicate on 1 ml of samples every two days, using an inverted light microscope.

2.2. Toxicity bioassays

Toxicity tests were performed on II–III stage larvae (nauplii) of the crustacean *Artemia salina* following the Artoxkit M, obtained from Microbiotest Inc. (Artoxkit, 1990), modified as in Faimali et al. (2012) during exponential, stationary and late stationary phases.

In order to investigate the toxic effect due to direct or indirect contact with *Ostreopsis* cf. *ovata* cells along the growth curve, nauplii of *Artemia salina* (15–20 organisms per 2 ml well) were exposed to: (A) untreated *O.* cf. *ovata* culture; (B) filtered (by 6 μm mesh size nylon net) and resuspended *O.* cf. *ovata* cells in fresh medium; (C) filtered, resuspended and sonicated *O.* cf. *ovata* cells in fresh medium; (D) growth medium devoid of algal cells by 0.22 μm mesh size filtration, where both cells and mucilaginous matrix were removed (GM 0.22 μm). All treatments (A–D) were tested with concentrations of 4, 40 and 400 cells/ml, at the three phases of the growth curve; three replicates were prepared for each combination of treatments and cell concentrations, including a control (CTR; 0.22 μm Filtered Natural Sea Water).

Moreover, during the late stationary phase, a further investigation was performed to elucidate the role of the mucilaginous matrix. The toxicity bioassay was replicated with treatments A, D and a new one E): growth medium obtained by filtration through a 6 μm mesh size nylon net, which allows the mucilaginous matrix pass through, but retains the cells. These treatments were tested at

the concentration of 400 cells/ml; three replicates were prepared for each treatment, including the control (0.22 μm Filtered Natural Sea Water).

Multiwell plates were stored at 20 °C with a 16:8 L:D cycle. After 48 h, the number of dead nauplii was observed under a stereomicroscope.

2.3. Statistical analysis

Three way crossed analysis of variance (three way-ANOVA) and Student-Newman-Keuls (SNK) tests were performed for the comparison of means to check for differences among mortality values for the first experimental setup. Factors tested were: Phase (exponential, stationary and late stationary; three levels), Concentration (4, 40, 400 cells/ml; three levels) and Treatment (A–D; four levels).

In the second experiment, testing effects of cells, mucous and growth medium during the late stationary phase, a one way-ANOVA was performed to test effects of factor Treatment (A, D, E; three levels).

All ANOVAs were performed after checking for homoscedasticity using the Cochran test.

The LC50–24 h and LC50–48 h values (the concentration of *Ostreopsis* cf. *ovata* cells causing 50% mortality after 24 and 48 h of exposure) were calculated using trimmed Spearman–Karber analysis (Finney, 1978).

2.4. Molecular analysis

To check possible presence of algal cells in the treatment E and, therefore, to better understand and validate the interpretation of the ecotoxicological bioassay, 60 ml of *Ostreopsis* cf. *ovata* culture (harvested during the late stationary phase) was filtered through a 6 μm mesh size nylon, replaced in a new sterilized plastic flask and analysed by qPCR assay.

In particular, the 6 μm fraction was filtered through a 25 mm diameter Durapore membrane with a pore size of 0.65 μm (Millipore, USA) under gentle vacuum in order to recover possible biological components. Then, the filter was transferred into a new 1.5 ml tube containing 500 μl of lysis buffer as described by Perini et al. (2011). Particulate material was washed out from the filter, the filter discharged and the suspension was lysed as described in detail by Casabianca et al. (2013). Briefly, after three freeze/thaw cycles the sample was incubated at 55 °C for 3 h and vortexed every 20 min. A 100 °C for 5 min step was performed to inactivate the proteinase K. Finally, the suspension was centrifuged at 12,000 rpm for 1 min to precipitate cell debris. The supernatant, or crude extract, was transferred into a new tube, and diluted at 1:10 and 1:100 for the qPCR experiments.

The 6 μm fraction, treated as described above, was analyzed by qPCR following the protocol of Perini et al. (2011) using primers for the amplification of 204 bp specific fragment targeting LSU rDNA of *Ostreopsis* cf. *ovata*. A plasmid (pLSUO) standard curve was constructed by amplifying 10-fold scalar dilutions with the copy number ranging from 1×106 to 1×102 (two replicates), and from 1×101 to 2×100 (four replicates).

A cellular standard curve was generated with dilutions from 8 to $8 \times 10 - 4$ lysed cells. The rDNA copy number per cell of *Ostreopsis* cf. *ovata* was calculated.

The qPCR assay was carried out in a final volume of 25 μl using the Hot-Rescue Real-Time PCR Kit-SG (Diatheva, Fano, Italy) in a StepOne Real-Time PCR System (Applied Biosystems, CA), primers at a final concentration of 200 nM, 0.5 U of Hot-Rescue Taq DNA polymerase, and 2 μl undiluted, 1:10 and 1:100 diluted of culture crude extract. Amplification reactions were carried out using a Step-one Real-time PCR System (Applied Biosystem, Foster City, CA, USA). The thermal cycling conditions consisted of 10 min at 95 °C, followed by 40 cycles at 95 °C for 15 s and 60 °C for 1 min.

Acquisition of qPCR data and subsequent analyses were carried out using StepOne software v. 2.3. A dissociation curve was generated, after each amplification run, to check for amplicon specificity and primers dimer formation. Results from 10-fold dilutions with a Ct difference between 3.3 and 3.4 (ΔCt of 3.3 corresponds to 100% efficiency) were accepted.

2.5. Chemical analysis

In order to characterize and quantify toxins produced by *Ostreopsis* cf. *ovata*, chemical analyses were performed at the University of Naples on aliquots of D (150 ml), E (175 ml) treatments and on *O.* cf. *ovata* cell pellet (about 1×106 cells arising from 175 ml culture containing round to 5400 cells/ml) collected during late stationary phase.

Cell pellets and growth media for each treatment were extracted separately as follows. Pellets were added to 30 ml of a methanol/water (1:1, v/v) solution and sonicated for 5 min in pulse mode, while cooling in ice bath. The mixture was centrifuged at 6500 rpm for 10 min; the supernatant was decanted and the pellet was extracted once again with 20 ml of the extraction solvent. The supernatant was decanted and the two extracts were combined (42 ml total). The obtained mixture was analyzed directly by LC-HRMS (5 μl injected). Growth media were extracted five times with an equal volume of butanol. The butanol layer was evaporated to dryness, dissolved in 8 ml of methanol/water (1:1, v/v) and analyzed directly by LC-HRMS (5 μl injected). Recovery percentages of the above extraction procedures were 98% for the pellet and 75% for the growth medium (Ciminiello et al., 2006).

LC-HRMS analyses were carried out on an Agilent 1100 LC binary system (Palo Alto, CA, USA) coupled to a hybrid linear ion trap LTQ Orbitrap XLTM Fourier Transform MS (FTMS) equipped with an ESI ION MAXTM source (Thermo-Fisher, San José, CA, USA). Chromatographic separation was accomplished on a 3 μm Gemini C18 (150×2.00 mm) column (Phenomenex, Torrance, CA, USA) maintained at room temperature and eluted at 0.2 ml min^{-1} with water (eluent A) and 95% acetonitrile/water (eluent B), both containing 30 mM acetic acid. A slow gradient elution was used: 20% to 50% B over 20 min, 50% to 80% B over 10 min, 80% to 100% B in 1 min, and hold for 5 min. This gradient system allowed a sufficient chromatographic separation of most palytoxin-like compounds with the only exception of ovatoxin-d and -e. HR full MS experiments (positive ions) were acquired in the range m/z 800–1400 at a resolving power of 60,000. The following source settings were used: a spray voltage of 47 V, a capillary temperature of 290 C°, a capillary voltage of 47 V, a sheath gas and an auxiliary gas flow of 38 and 2 (arbitrary units). The tube lens voltage was set at 105 V.

Identification of palytoxin-like compounds contained in the extracts was made on the basis of retention time, elemental formula of the most intense doubly- and triply-charged ions (mono-isotopic ion peak) contained in full HRMS spectrum, and isotopic pattern of each ion cluster. An *Ostreopsis* cf. *ovata* extract previously characterized (Pezzolesi et al., 2012) was used as reference sample. HR collision induced dissociation (CID) LC-MS2 experiments were carried out to confirm the identity of individual toxins as reported previously (Ciminiello et al., 2010, 2012a,b). Extracted ion chromatograms (XIC) were obtained for each palytoxin-like compound by selecting the most abundant ion peaks of both $[M + 2H\text{-}H2O]^{2+}$ and $[M + H + Ca]^{3+}$ ion clusters at a mass tolerance of 5 ppm. Due to commercial availability of the only palytoxin standard, quantitation of the palytoxin-like compounds was carried out by assuming that their molar responses were similar to that of palytoxin. Calibration curve (triplicate injection)

of palytoxin standard at four levels of concentration (1000, 100, 50, and 12.5 ng ml^{-1}) was used. Calibration curve equation was $y = 10461.3160 \times 232615.2993$ and its linearity was expressed by $R^2 = 0.997$.

2.6. Atomic force microscopy (AFM)

A 20 μl drop of *Ostreopsis* cf. *ovata* culture was deposited directly onto clean glass substrate overnight to allow cells settle and adhere to the surface. Samples were then rinsed in ultrapure water to remove the excess of salt crystals and then placed in Petri dish to allow the excess of water to evaporate. As a consequence of the rinsing procedure the cells disaggregated, breaking down into the separate plates. Stable AFM imaging of the thecal plates, firmly adhered to the glass sheet were then performed. Data acquisition was carried out by using a custom build AFM head (Pini et al., 2010) based on a three axis closed loop flexure scanner with travel ranges 200 × 200 × 20 μm (mod. PI—527.3CL, Physik Instrumente, Karlsruhe, Germany) and driven by R9 digital controller by RHK Technology – Troy, MI (USA), in intermittent contact mode in air at room temperature. Rectangular silicon cantilevers (PPP-NCHR, Nanosensors, Neuchatel, Switzerland) with a nominal tip radius of 10 nm and 330 kHz resonance frequency were used. Topography images were acquired at a resolution of 512 pixels per line using a scan rate of 0.4 Hz. AFM scanner performance and calibration were routinely checked by using a reference grid model STR3-180P (VLSI Standards, CA, U.S.A.) with a lateral pitch of 3 μm and step height of 18 nm. AFM images were pre-processed for tilt correction and scars removal with Gwyddion software.

3. Results

3.1. Toxicity bioassay

Mortality of *Artemia salina* nauplii exposed for 48 h to A, B, C and D treatments performed along exponential, stationary and late stationary phases are shown in Fig. 1(a–c). In general, our data show that the toxicity of *Ostreopsis* cf. *ovata* increases during the growth curve, causing the higher mortality values during the late stationary phase. In particular, as far as the lower concentrations tested (4 and 40 cells/ml) of untreated *O.* cf. *ovata* culture (A treatment), statistical comparison among the three growth curve phases demonstrates a significantly higher toxic effect during the late stationary phase ($p < 0.01$), with mortality values exceeding 80%. These findings are supported also by the decrease in LC50–48 h values: 25 cells/ml during the exponential phase, 17 cells/ml during the stationary phase and < 4 cells/ml during the late stationary phase. The same decreasing trend of LC50–48 h values along the three phases of the growth curve is also observed in the B (resuspended *O.* cf. *ovata* cultures) and C (sonicated culture)

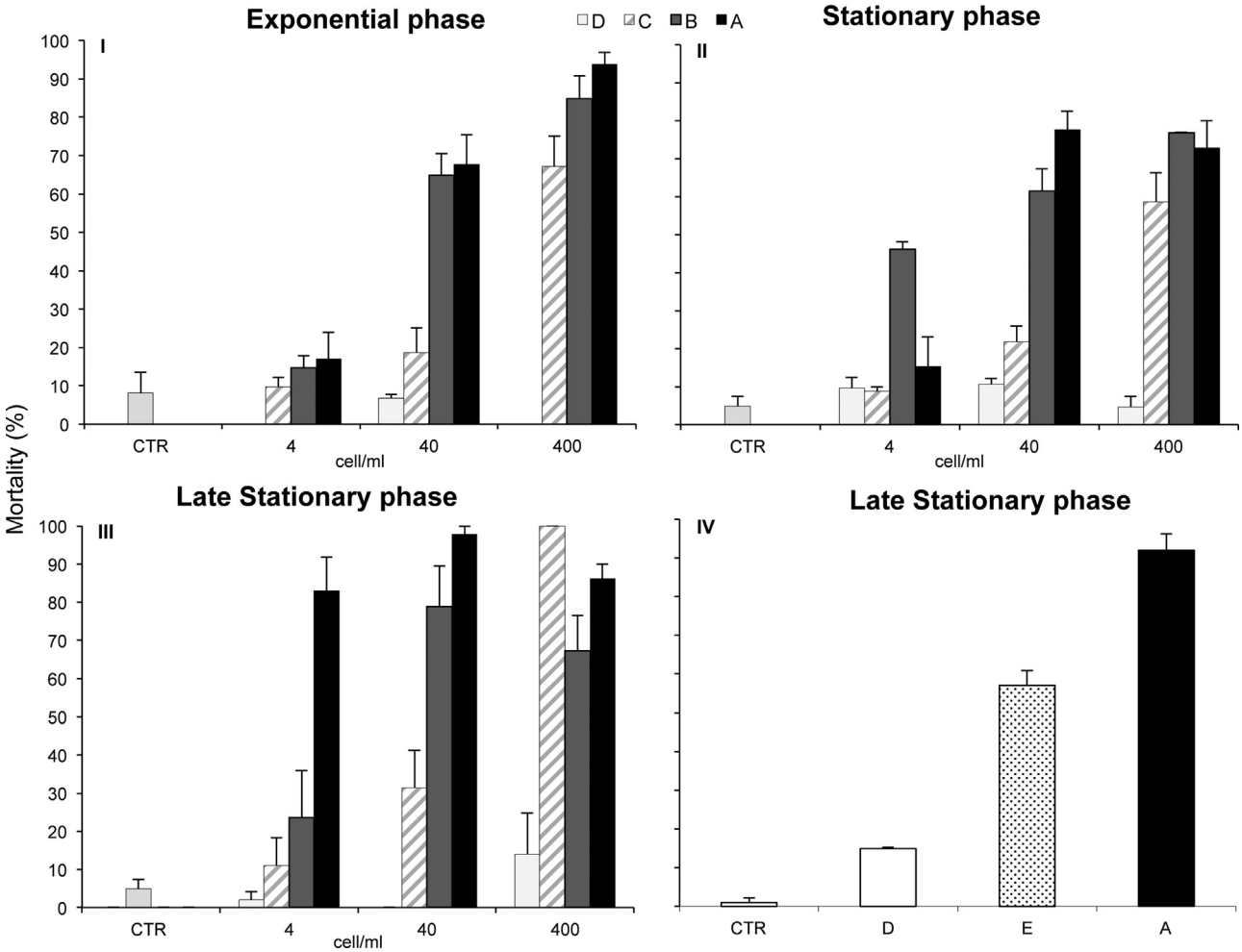

Fig. 1. Mortality (avg ± standard error, $N = 3$) of *Artemia salina* after 48 h of exposure to 0.22 μm filtered growth medium (D; white bar), sonicated *O.* cf. *ovata* culture (C; striped bar), resuspended *O.* cf. *ovata* culture (B; grey bar) and untreated *O.* cf. *ovata* culture (A; black bar), during exponential (I), stationary (II) and late stationary (III) phases of the growth curve; IV) mortality (avg ± standard error, $N = 3$) of *Artemia salina* after 48 h exposure to 0.22 μm filtered growth medium (D), 6 μm filtered growth medium (E) and untreated *O.* cf. *ovata* culture (A), at the concentration of 400 cells/ml during the late stationary phase. CTR: control in filtered natural seawater.

Table 1
LC50-48 h values (cells/ml) and confidence limits obtained exposing nauplii of *A. salina* to A) untreated *O.* cf. *ovata* culture, B) resuspended *O.* cf. *ovata* culture, C) sonicated *O.* cf. *ovata* culture and D) 0.22 μm filtered growth medium, during exponential, stationary and late stationary phases of algal growth curve.

Treatments	LC 50–48 h (cells/ml)		
	Exponential phase	Stationary phase	Late stationary phase
A	24.83 (18.59–33.16)	16.67 (13.46–20.63)	< 4 cell/ml
B	30.12 (20.92–43.37)	10.19 (3.86–26.91)	15.26 (11.56–20.15)
C	214.40 (155.96–294.75)	266.92 (163.64–435.39)	65.48 (51.23–83.68)
D	>400	>400	>400

treatments (Table 1). Effects are stronger in A (untreated culture) and B treatments, while C treatment displays higher percentage of mortality (67%, 59% and 100%, during exponential, stationary and late stationary phases, respectively) only at the highest tested concentration (400 cells/ml).

Growth medium devoid of both algal cells and mucilaginous matrix by 0.22 μm mesh size filtration (treatment D) did not show any relevant toxic effect among any concentrations tested throughout all growth curve phases.

Results from the toxicity bioassay performed during the late stationary phase to disentangle the effects of direct contact with cells and the mucous filaments are reported in Fig. 1d. Also in this case the 0.22 μm filtered growth medium (D treatment) does not show relevant mortality effects, while the growth medium obtained by filtration through 6 μm mesh size nylon net registered almost 60% mortality (57.8%, $p < 0.01$).

3.2. Molecular analysis

The comparison of the pLSUO and cellular standard curves showed the same efficiency (98−100% and $\Delta s < 0.1$, data not shown), thus it was possible to calculate the rDNA copy number per cell of *Ostreopsis* cf. *ovata*. The normalized copy per cell of *O.* cf. *ovata* was 2859 ± 175 (Ct mean = 22.95 ± 0.09). The 6 μm filtered growth medium was analyzed by qPCR and was positive for the presence of few *O.* cf. *ovata* cells. In particular, the Ct mean value was 29.39 ± 0.12 ($n = 3$) corresponding to 8243 ± 658 total LSU rDNA copy number. Thus, only three cells were quantified in the 6 μm filtered growth medium.

3.3. Chemical analyses: determination of toxin profile and content

Crude extracts of cell pellets and growth media for each treatment (D and E treatments) were directly analyzed by LC-HRMS using a slow gradient elution (Ciminiello et al., 2010), which allowed to chromatographically separate most of the components of the toxin profile. Full HR MS spectra were acquired in the mass range m/z 800–1400 where each palytoxin-like compound produced dominant doubly and triply-charged ions due to $[M + 2H\text{-}H2O]^{2+}$ and $[M + H + Ca]^{3+}$, respectively (Ciminiello et al., 2011). Under such conditions, accurate quantitation was possible for most of the palytoxin-like compounds produced by *Ostreopsis* cf. *ovata*, with the only exception of the structural isomers ovatoxin-d and–e, which were quantified as sum. Instrumental limit of detection for palytoxin was 3.12 ng ml^{-1}. Based on extraction volume, the presence of toxins in pellet (1 × 106 cells), growth medium D (150 ml), and E (175 ml) could be estimated at levels ≥ 0.13 pg/cell, 0.17, and 0.14 μg/l, respectively.

An Adriatic *Ostreopsis* cf. *ovata* extract previously characterized (Pezzolesi et al., 2012) was analyzed in parallel under the same experimental conditions and used as reference samples. Palytoxin standard was used in quantitative studies assuming that toxins produced by *O.* cf. *ovata* present the same molar response as palytoxin, which seems quite reasonable based on structural similarities.

Unlike the *Ostreopsis* cf. *ovata* reference sample, extracts of pellet and 6 μm filtered growth medium (E) extract contained only ovatoxin-a, ovatoxin-d and -e and a putative palytoxin, while ovatoxin-b and -c were not detected. No palytoxin-like compound was detected in 0.22 μm filtered growth medium (D). Total toxin content on a per cell basis was 44 pg/cell (pellet), with ovatoxin-a being the major component of the toxin profile (76%), followed by ovatoxin-d and -e (21%) and pPLTX (3%). The highest toxin content was measured in pellet extract (95%) with only 5% being measured in the 6 μm growth medium, while toxins were not detected in the 0.22 μm medium (Table 2).

3.4. Atomic force microscope

Innovative characterization of the inner side of *Ostreopsis* cf. *ovata* thecal plates, performed by AFM without staining and fissative treatments, is shown in Fig. 2. Our investigation highlighted three cellulose layers of the hypothecal plates (specifically on 3‴ plate, Fig. 2b), resulting in 460 nm (for the two inner ones) and 740 nm (for the external one) of thickness. Thecal plates display scattered pores of around 230 nm average diameter ($N = 65$): on the inner side of the plates, differently from the smooth outer side, the pores are surrounded by a raised edge (around 65 nm height). Moreover, some pores are covered by a conical structure from which channels and filaments (230 nm thick; Fig. 2c) depart, suggesting that these are structural parts involved in the extrusion mechanism of trichocysts.

4. Discussion

The chemical analyses on the *Ostreopsis* cf. *ovata* strain investigated in the present study show that toxin profile of the culture differs from that usually found in Mediterranean *O.* cf. *ovata* strains from both a qualitative and quantitative standpoint; more in details, it did not contain ovatoxin-b and -c, versus a previously characterized Adriatic *O.* cf. *ovata* strain containing

Table 2
Toxin content of pellet (pg/cell and μg/l), 6 μm filtered (E) and 0.22 μm filtered (D) growth medium of *O.* cf. *ovata* culture. Conversion between pg/cell and mg/l is calculated according to the cell concentration of 5.40 × 103 cells/ml.

Toxin	Pellet (pg/cell)	Pellet (μg/l)	Medium 6 μm (μg/l)	Medium 0.22 μm (μg/l)
Ovatoxin-a	33.5	180.9	8.0	nd
Ovatoxin-d and -e	9.0	51.3	4.0	nd
Putative palytoxin	1.5	8.5	Trace	nd
Total toxin content	44	240.7	12	nd

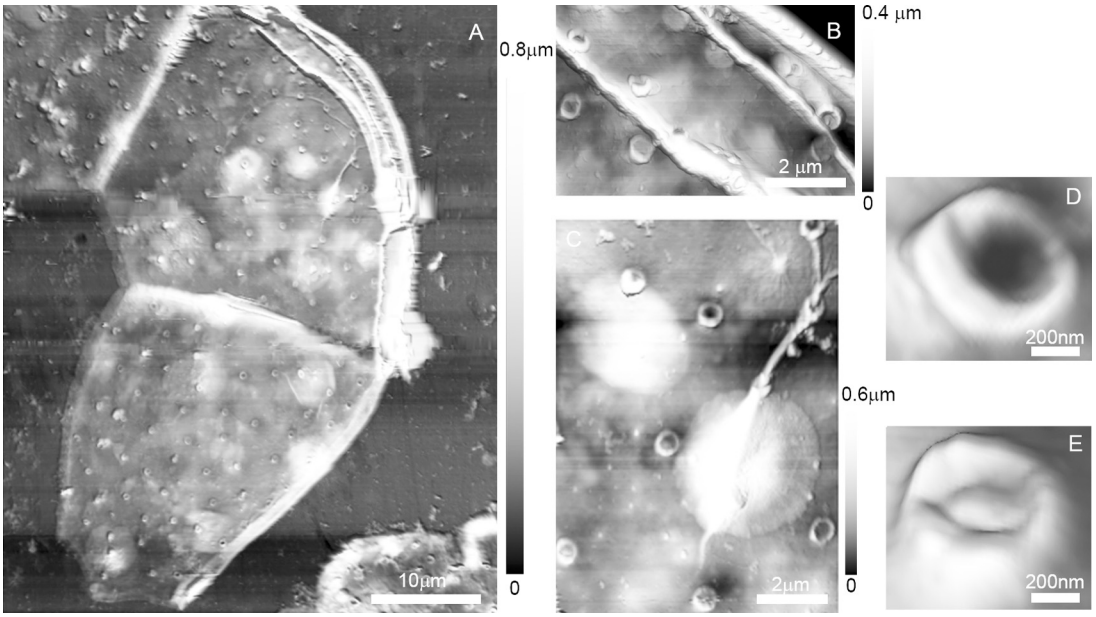

Fig. 2. (a) Overview of the inner side of *Ostreopsis* cf. *ovata* hypotheca obtained by atomic force microscopy (AFM); (b) zoom on the three cellulose layers of the thecal plate; (c) trichocyst and thecal pores on inner side of 3‴ thecal plate; (d)–(e) blowup of thecal pores.

ovatoxin-a (56%), -b (24%), -d and -e (15%), -c (4%), and putative palytoxin (1%). A similar toxin profile has been reported by Ciminiello et al. (2012a,b) in only one Adriatic *O.* cf. *ovata* strain. The variability in toxin profile of different isolates of this species (Pistocchi et al., 2011) is stressed by intrinsic (e.g. different strains) and extrinsic (e.g. different habitat) factors (GEOHAB, 2012), that can influence not only toxicity but also amount of mucilage produced.

This study reports increasing ecotoxicological effects of *Ostreopsis* cf. *ovata* along its growth curve, with LC50 values of *Artemia salina* lower at the late stationary phase.

The ecotoxicological bioassay provides additional evidence that not only toxin production increases along the growth curve, as reported in literature (Guerrini et al., 2010), but also toxic effects on model organisms are more severe. In fact, several studies, mainly focusing on toxin quantification and characterization, report that toxicity of *Ostreopsis* cf. *ovata*, as for other benthic dinoflagellates, increases along the growth curve, reaching the highest toxin content in the cells at the end of the stationary phase (Granéli et al., 2011; Vidyarathna and Granéli, 2012).

In addition to the increase in toxicity effects along the growth curve, more interestingly, our study shows that toxicity effects on model organisms change drastically according to the presence or not of living cells or mucous filaments. So far, toxicity mechanisms of *Ostreopsis* spp. are still unclear. Faimali et al. (2012) already observed that toxic effects on marine invertebrates occurred only when they were exposed to direct contact of intact microalgal cells (LC50-48 h at 20 and 25 °C of whole culture equal to 12.43 and < 4 cells ml^{-1}, while LC50-48 h at 20–25 °C of 0.22 μm filtered growth medium were around 4000 cell/ml, respectively). Moreover, similar trend of toxicity on *Artemia salina* nauplii and juveniles of sea basses has been demonstrated in Pezzolesi et al. (2012) which show EC50-24 h value of growth medium corresponding to 720 cells/ml versus 8 cells/ml with live cells.

The present study investigates the role of contact with living cells in conveying toxins to the organisms, discriminating between the contact with the whole cells and with the only mucous filaments produced by *Ostreopsis* cf. *ovata*. Honsell et al. (2013) described *O.* cf. *ovata* mucilage as a network of a very high number of trichocysts embedded with acidic polysaccharides filaments, both secreted through thecal pores, that generate a very resistant extracellular matrix never observed before among microalgal species. This matrix can be extremely thick, especially during the late bloom, when mass mortalities of marine organisms are usually recorded (Ferreira, 2006; Nascimento et al., 2012).

The potential toxic effects of both growth medium and mucilage were tested during the late stationary phase. The results of this test provide the first evidence of a significant toxic effect ($p < 0.01$) on *Artemia salina* after exposition to growth medium (devoid of microalgal cells) containing only *Ostreopsis* cf. *ovata* mucilage. Although previous findings report an increase in toxin content in the growth medium at the late stationary phase, possibly due to the large number of broken cells (Guerrini et al., 2010), our results on the 0.22 μm filtered growth medium show low mortality values at the late stationary phase as well as undetectable toxin concentrations by way of chemical analyses. On the contrary, 5% of toxins of the whole culture is present in the 6 μm growth medium, suggesting that toxins are retained in the mucous matrix.

Additional confirmation of the direct involvement of cells (or their filaments) in conveying toxicity to model organisms is provided by the evidence that the sonicated *Ostreopsis* cf. *ovata* culture, at a concentration comparable to those that often occur in nature ($\leq$40 cells/ml), had much lower effects than the intact cells. Only at the highest tested concentration (400 cells/ml, rarely found in nature) a remarkable toxic effect was observed. However, we cannot exclude that sonication may alter the molecular and toxicity properties (Faimali et al., 2012).

Our findings provide additional insights on the role of the microalgal mucilaginous matrix, that may represent a defense against grazing, a predation method to capture larger organisms by heterotrophic dinoflagellates (Kiørboe and Titelman, 1998; Barone and Prisanzano, 2006) and/or an adaptation to live in different benthic habitats (Totti et al., 2010; Parsons et al., 2012). But, most of all, as reported for other microalgal species (Blossom et al., 2012), *Ostreopsis* mucus could be a vehicle through which toxins are released into external medium and/or disseminated into the prey. In fact, the first observed effect on several marine organisms is the interlocking within the mucous (Shears and Ross, 2010; Privitera et al., 2012).

The possibly active role of the filaments in conveying toxicity is supported by the innovative images of the *Ostreopsis* cf. *ovata* theca obtained by atomic force microscopy. AFM images show scattered pores having different structure from their external one (as suggested also in Penna et al., 2005) and, at a higher magnification, highlight conical-tubular structures involved in the trychocyst extrusion mechanism.

5. Conclusions

The present study has provided additional evidence on the variability of the toxin profile of *Ostreopsis* cf. *ovata* strains, highlighting that: (i) the toxicity increases along the growth curve; (ii) negligible amounts of toxins are released in the growth medium and (iii) the mucous filaments play a direct, possibly active, role in conveying toxicity. In fact, the mucous matrix interlocks the organisms, enhances the surface of the contact area, and, most possibly, actively disseminates toxins.

Atomic force microscopy, providing new perspectives on ultrastructure investigations, seems to be a promising technique to highlight cellular features, their connections and role in *Ostreopsis* cf. *ovata*, and, in general, in other microalgae species (Morris et al., 1999; Radić et al., 2011; Mandal et al., 2011; Pletikapić et al., 2012).

Acknowledgments

This publication has been produced with the financial assistance of the European Union under the ENPI CBC Mediterranean Sea Basin Programme (M3-HABs project). The contents of this document are the sole responsibility of the authors and can under no circumstances be regarded as reflecting the position of the European Union or of the Programme's management structures. Chemical analyses were carried out in the framework of the STAR Programme, financially supported by University of Naples and Compagnia di San Paolo. Financial support was additionally provided by the Regione Liguria FAS 2007-2013 Programme (Project OVmeter). Thanks to Dr. Samuela Capellacci for isolating *Ostreopsis* strains.[SS]

References

Accoroni, S., Romagnoli, T., Pichierri, S., Colombo, F., Totti, C., 2012. Morphometric analysis of *Ostreopsis* cf *ovata* cells in relation to environmental conditions and bloom phases. Harmf. Algae 19, 15–22.

Aligizaki, K., Nikolaidis, G., 2006. The presence of the potentially toxic genera *Ostreopsis* and Coolia (Dinophyceae) in the North Aegean Sea, Greece. Harmf. Algae 5, 717–730.

Asnaghi, V., Bertolotto, R., Giussani, V., Mangialajo, L., Hewitt, J., Thrush, S., Moretto, P., Castellano, M., Rossi, A., Povero, P., Cattaneo-Vietti, R., Chiantore, M., 2012. Interannual variability in *Ostreopsis ovata* bloom dynamic along Genoa coast (North-western Mediterranean): a preliminary modeling approach. Cryptogam. Algol. 33 (2), 181–189.

Barone, R., 2007. Behavioural trait of Ostreopsis ovata (Dinophyceae) in Mediterranean rock pools: the spider's strategy. Harmful algae news.

Barone, R., Prisanzano, A., 2006. Peculiarita comportamentale del dinoflagellato *Ostreopsis ovata* Fukuyo (Dinophyceae): la strategia del ragno. Nat. Sicil. 30, 401–418.

Besada, E.G., Loeblich, L.A., Loeblich, A.R., 1982. Coral reef paper observ ations on tropical, benthic dinoflagellates from ciguatera-endemic areas: Coolia, Gambierdiscus, and *Ostreopsis*. Bull. Mar. Sci. 32, 723–735.

Blossom, H.E., Daugbjerg, N., Hansen, P.J., 2012. Toxic mucus traps: a novel mechanism that mediates prey uptake in the mixotrophic dinoflagellate *Alexandrium pseudogonyaulax*. Harmf. Algae 17, 40–53.

Brescianini, C., Grillo, C., Melchiorre, N., Bertolotto, Ferrari, R.A., Vivaldi, B., Icardi, G., Gramaccioni, L., Funari, E., Scardala, S., 2006. Ostreopsis ovata algal blooms affecting human health in Genova, Italy, 2005 and 2006. Euro Surveill 11 (9), E060907.

Casabianca, S., Casabianca, A., Riobó, P., Franco, J.M., Vila, M., Penna, A., 2013. Quantification of the toxic dinoflagellate *Ostreopsis* spp. by qPCR assay in marine aerosol. Environ. Sci Tech. 47, 3788–3795.

Ciminiello, P., Dell'Aversano, C., Dello Iacovo, E., Fattorusso, E., Forino, M., Grauso, L., Tartaglione, L., Guerrini, F., Pistocchi, R., 2010. Complex palytoxin-like profile of *Ostreopsis ovata*. Identification of four new ovatoxins by high-resolution liquid chromatography/mass spectrometry. Rapid Commun. Mass Spectrom. 24, 2735–2744.

Ciminiello, P., Dell'Aversano, C., Fattorusso, E., Forino, M., Magno, G.S., Tartaglione, L., Grillo, C., Melchiorre, N., 2006. The Genoa 2005 Outbreak. Determination of Putative Palytoxin in Mediterranean Ostreopsis o vata by a New Liquid Chromatography Tandem Mass Spectrometry Method. Analytical chemistry 78 (17), 6153–6159.

Ciminiello, P., Dell'Aversano, C., Dello Iacovo, E., Fattorusso, E., Forino, M., Grauso, L., Tartaglione, L., Guerrini, F., Pezzolesi, L., Pistocchi, R., Vanucci, S., 2012a. Isolation and structure elucidation of ovatoxin-a, the major toxin produced by *Ostreopsis ovata*. J. Am. Chem. Soc. 134, 1869–1875.

Ciminiello, P., Dell'Aversano, C., Dello Iacovo, E., Fattorusso, E., Forino, M., Tartaglione, L., 2011. LC-MS of palytoxin and its analogues: State of the art and future perspectives. Toxicon 57 (3), 376–389.

Ciminiello, P., Dell'Aversano, C., Iacovo, E., Dello, Fattorusso, E., Forino, M., Tartaglione, L., Battocchi, C., Crinelli, R., Carloni, E., Magnani, M., Penna, A., 2012b. Unique toxin profile of a Mediterranean *Ostreopsis* cf. *ovata* strain: HR LC-MS(n) characterization of ovatoxin-f, a new palytoxin congener. Chem. Res. Toxicol. 25, 1243–1252.

Escalera, L., Benvenuto, G., Scalco, E., Zingone, A., Montresor, M., 2014. Ultrastructural features of the benthic dinoflagellate *Ostreopsis* cf. *ovata* (Dinophyceae). Protist 165 (3), 260–274.

Faimali, M., Giussani, V., Piazza, V., Garaventa, F., Corrà, C., Asnaghi, V., Privitera, D., Gallus, L., Cattaneo-Vietti, R., Mangialajo, L., Chiantore, M., 2012. Toxic effects of harmful benthic dinoflagellate *Ostreopsis ovata* on invertebrate and vertebrate marine organisms. Mar. Environ. Res. 76, 97–107.

Ferreira, C.E.L., 2006. Sea urchins killed by toxic algae. JMBA Glob. Mar. Environ. 3, 22–23.

Finney, D.J., 1978. Statistical Method in Biological Assay, third ed. Charles Griffin & Co. Ltd, London, England, p. 508.

GEOHAB, 2012. GEOHAB core research project: HABs in benthic systems. Organization 64.

Granéli, E., Ferreira, C., Yasumoto, T., Rodrigues, E., Neves, B., 2002. Sea urchins poisoning by the benthic dinoflagellate Ostreopsis ovata on the Brazilian Coast. In: Steidinger, K.A. (Ed.), Book of Abstracts 10th Int Conf on Harmful Algae, 21–25. St. Pete Beach, FL, p. 113.

Granéli, E., Vidyarathna, N.K., Funari, E., Cumaranatunga, P.R.T., Scenati, R., 2011. Can increases in temperature stimulate blooms of the toxic benthic dinoflagellate *Ostreopsis ovata*. Harmf. Algae 10 (2), 165–172.

Grzebyk, D., Denardou, A., Berland, B., Pouchus, Y.F., 1997. Evidence of a new toxin in the red-tide dinoflagellate *Prorocentrum minimum*. J. Plankton Res. 19 (8), 1111–1124.

Guerrini, F., Pezzolesi, L., Feller, A., Riccardi, M., Ciminiello, P., Dell'Aversano, C., Tartaglione, L., Dello Iacovo, E., Fattorusso, E., Forino, M., Pistocchi, R., 2010. Comparative growth and toxin profile of cultured *Ostreopsis ovata* from the Tyrrhenian and Adriatic Seas. Toxicon. 55, 211–220.

Honsell, G., Bonifacio, A., De Bortoli, M., Penna, A., Battocchi, C., Ciminiello, P., Dell'aversano, C., Fattorusso, E., Sosa, S., Yasumoto, T., Tubaro, A., 2013. New insights on cytological and metabolic features of *Ostreopsis* cf. *ovata* Fukuyo (Dinophyceae): a multidisciplinary approach. PLOS ONE 8, e57291.

Hwang, B.S., Yoon, E.Y., Kim, H.S., Yih, W., Park, J.Y., Jeong, H.J., Rho, J.-R., Ostreol, A., 2013. A new cytotoxic compound isolated from the epiphytic dinoflagellate *Ostreopsis* cf. *ovata* from the coastal waters of Jeju Island. Korea. Bioorg. Med. Chem. Lett. 23, 3023–3027.

Kiørboe, T., Titelman, J., 1998. Feeding, prey selection and prey encounter mechanisms in the heterotrophic dinoflagellate *Noctiluca scintillans*. J. Plankton Res. 20, 1615–1636.

Liu, H., Buskey, E.J., 2000. Hypersalinity enhances the production of extracellular polymeric substance (EPS) in the Texas brown tide alga, *Aureoumbra lagunensis* (Pelagophyceae). J. Phycol. 36 (1), 71–77.

Mandal, S.K., Singh, R.P., Patel, V., 2011. Isolation and characterization of exopolysaccharide secreted by a toxic dinoflagellate, *Amphidinium carterae* Hulburt 1957 and its probable role in harmful algal blooms (HABs). Microb. Ecol. 62 (3), 518–527.

Mangialajo, L., Bertolotto, R., Cattaneo-Vietti, R., Chiantore, M., Grillo, C., Lemee, R., Melchiorre, N., Moretto, P., Povero, P., Ruggieri, N., 2008. The toxic benthic dinoflagellate *Ostreopsis ovata*: quantification of proliferation along the coastline of Genoa. Italy. Mar. Pollut. Bull. 56, 1209–1214.

Mangialajo, L., Ganzin, N., Accoroni, S., Asnaghi, V., Blanfuné, A., Cabrini, M., Cattaneo-Vietti, R., Chavanon, F., Chiantore, M., Cohu, S., Costa, E., Fornasaro, D., Grossel, H., Marco-Miralles, F., Maso, M., Rene, A., Rossi, A.M., Montserat Sala, M., Thibaut, T., Totti, C., Vila, M., Lemée, R., 2011. Trends in *Ostreopsis* proliferation along the Northern Mediterranean coasts. Toxicon. 57, 408–420.

Morris, V.J., Kirby, A.R., Gunning, A.P., 1999. Atomic Force Microscopy for Biologist. Imperial College Press, London.

Munday, R., 2011. Palytoxin toxicology: animal studies. Toxicon. 57, 470–477.

Nascimento, S.M., França, J.V., Gonçalves, J.E., Ferreira, C.E., 2012. *Ostreopsis* cf. *ovata* (Dinophyta) bloom in an equatorial island of the Atlantic Ocean. Mar. Pollut. Bull. 64 (5), 1074–1078.

Parsons, M.L., Aligizaki, K., Bottein, M.-Y.D., Fraga, S., Morton, S.L., Penna, A., Rhodes, L., 2012. Gambierdiscus and *Ostreopsis*: reassessment of the state of knowledge of their taxonomy, geography, ecophysiology, and toxicology. Harmf. Algae 14, 107–129.

Penna, A., Fraga, S., Battocchi, C., Casabianca, S., Giacobbe, M.G., Riobo, P., Vernesi, C., 2010. A phylogeographical study of the toxic benthic dinoflagellate genus *Ostreopsis* Schmidt. J. Biogeogr. 37, 841 L-380.

Penna, A., Vila, M., Fraga, S., Giacobbe, M.G., Andreoni, F., Riobó, P., Vernesi, C., 2005. Characterization of *Ostreopsis* and *Coolia* (Dinophyceae) isolates in the Western Mediterranean sea based on morphology, toxicity and Internal Transcribed Spacer 5.8 S rDNA sequences1. Journal of phycology 41 (1), 212–225.

Perini, F., Casabianca, A., Battocchi, C., Accoroni, S., Totti, C., Penna, A., 2011. New approach using the real-time PCR method for estimation of the toxic marine dinoflagellate *Ostreopsis* cf. *ovata* in marine environment. PLoS ONE 6 (3), e17699.

Pezzolesi, L., Guerrini, F., Ciminiello, P., Dell'Aversano, C., Iacovo, E.D., Fattorusso, E., Pistocchi, R., 2012. Influence of temperature and salinity on *Ostreopsis* cf. *ovata* growth and evaluation of toxin content through HR LC-MS and biological assays. Water Res. 46 (1), 82–92.

Pini, V., Tiribilli, B., Gambi, C.M.C., Vassalli, M., 2010. Dynamical characterization of vibrating afm cantilevers forced by photothermal excitation. Physical Rev. B 81 (5), 054302.

Pistocchi, R., Pezzolesi, L., Guerrini, F., Vanucci, S., Dell'Aversano, C., Fattorusso, E., 2011. A review on the effects of environmental conditions on growth and toxin production of *Ostreopsis ovata*. Toxicon. 57, 421–428.

Pletikapić, G., Berquand, A., Radić, T.M., Svetličić, V., 2012. Quantitative nanomechanical mapping of marine diatom in seawater using peak force tapping atomic force microscopy. J. Phycol. 48 (1), 174–185.

Privitera, D., Giussani, V., Isola, G., Faimali, M., Piazza, V., Garaventa, F., Asnaghi, V., Cantamessa, E., Cattaneo-Vietti, R., Chiantore, M., 2012. Toxic effects of *Ostreopsis ovata* on larvae and juveniles of *Paracentrotus lividus*. Harmf. Algae 18, 16–23.

Radić, T.M., Svetličić, V., Žutić, V., Boulgaropoulos, B., 2011. Seawater at the nanoscale: marine gel imaged by atomic force microscopy. J. Mol. Recognit. 24 (3), 397–405.

Ramos, V., Vasconcelos, V., 2010. Palytoxin and analogs: biological and ecological effects. Mar. Drugs 8, 2021–2037.

Reynolds, C.S., 2006. Ecology of Phytoplankton. Cambridge University Press, Cambridge, p. 535.

Reynolds, C.S., 2007. Variability in the provision and function of mucilage in phytoplankton: facultative responses to the environment. Hydrobiologia 578, 37–45.

Rhodes, L., 2011. World-wide occurrence of the toxic dinoflagellate genus *Ostreopsis* Schmidt. Toxicon. 57, 400–407.

Richlen, M.L., Morton, S.L., Barber, P.H., 2011. Phylogeography, morphological variation and taxonomy of the toxic dinoflagellate *Gambierdiscus toxicus* (Dinophyceae). Harmf. Algae 7, 614–629.

Shears, N.T., Ross, P.M., 2009. Blooms of benthic dinoflagellates of the genus *Ostreopsis*: an increasing and ecologically important phenomenon on temperate reefs in New Zealand and worldwide. Harmf. Algae 8, 916–925.

Shears, N.T., Ross, P.M., 2010. Toxic cascades: multiple anthropogenic stressors have complex and unanticipated interactive effects on temperate reefs. Ecol. Lett. 13, 1149–1159.

Tosteson, T.R., 1995. The diversity and origins of toxins in ciguatera fish poisoning. P. R. Health Sci. J. 14, 117–129.

Totti, C., Accoroni, S., Cerino, F., Cucchiari, E., Romagnoli, T., 2010. *Ostreopsis ovata* bloom along the Conero Riviera (Northern Adriatic Sea): relationships with environmental conditions and substrata. Harmf. Algae 9, 233–239.

Vidyarathna, N.K., Granéli, E., 2012. Influence of temperature on growth, toxicity and carbohydrate production of a Japanese *Ostreopsis ovata* strain, a toxic-bloom-forming dinoflagellate. Aquat. Microb. Ecol. 65 (3), 261–270.

Vila, M., Masó, M., Sampedro, N., Illoul, H., Arin, L., Garcés, E., Giacobbe, M.G., Alvarez, J., Camp, J., 2008. The genus Ostreopsis in recreational waters of the Catalan Coast and Balearic Islands (NW Mediterranean Sea): is this the origin of human respiratory difficulties?.

Vila, M., Garcés, E., Masó, M., 2001. Potentially toxic epiphytic dinoflagellate assemblages on macroalgae in the NW Mediterranean. Aquat. Microb. Ecol. 26, 51–60.